nature medicine

SUPPLEMENTARY INFORMATION

https://doi.org/10.1038/s41591-020-0770-2

In the format provided by the authors and unedited.

Dynamic imaging in patients with tuberculosis reveals heterogeneous drug exposures in pulmonary lesions

Alvaro A. Ordonez[1,2,3], Hechuan Wang[4], Gesham Magombedze[5], Camilo A. Ruiz-Bedoya[1,2,3], Shashikant Srivastava[5], Allen Chen[1,6], Elizabeth W. Tucker[1,2,7], Michael E. Urbanowski[2,8], Lisa Pieterse[1,2,7], E. Fabian Cardozo[9], Martin A. Lodge[6], Maunank R. Shah[2,8], Daniel P. Holt[6], William B. Mathews[6], Robert F. Dannals[6], Jogarao V. S. Gobburu[4], Charles A. Peloquin[10], Steven P. Rowe[6], Tawanda Gumbo[5], Vijay D. Ivaturi[4] and Sanjay K. Jain[1,2,3,6] ✉

[1]Center for Infection and Inflammation Imaging Research, Johns Hopkins University School of Medicine, Baltimore, MD, USA. [2]Center for Tuberculosis Research, Johns Hopkins University School of Medicine, Baltimore, MD, USA. [3]Department of Pediatrics, Johns Hopkins University School of Medicine, Baltimore, MD, USA. [4]Center for Translational Medicine, University of Maryland School of Pharmacy, Baltimore, MD, USA. [5]Center for Infectious Diseases Research and Experimental Therapeutics, Baylor University Medical Center and Texas Tech University Health Sciences Center, Dallas, TX, USA. [6]Russell H. Morgan Department of Radiology and Radiological Sciences, Johns Hopkins University School of Medicine, Baltimore, MD, USA. [7]Department of Anesthesiology and Critical Care Medicine, Johns Hopkins University School of Medicine, Baltimore, MD, USA. [8]Department of Medicine, Johns Hopkins University School of Medicine, Baltimore, MD, USA. [9]Vaccine and Infectious Disease Division, Fred Hutchinson Cancer Research Center, Seattle, WA, USA. [10]Infectious Disease Pharmacokinetics Laboratory, Pharmacotherapy and Translational Research, University of Florida College of Pharmacy, Gainesville, FL, USA. ✉e-mail: sjain5@jhmi.edu

Supplementary information

Dynamic Imaging in Tuberculosis Patients Reveals Heterogeneous Drug Exposures in Pulmonary Lesions

Alvaro A. Ordonez[1,2,3], Hechuan Wang[4], Gesham Magombedze[5], Camilo A. Ruiz-Bedoya[1,2,3], Shashikant Srivastava[5], Allen Chen[1,6], Elizabeth W. Tucker[1,2,7], Michael E. Urbanowski[2,8], Lisa Pieterse[1,2,7], E. Fabian Cardozo[9], Martin A. Lodge[6], Maunank R. Shah[2,8], Daniel P. Holt[6], William B. Mathews[6], Robert F. Dannals[6], Jogarao V. S. Gobburu[4], Charles A. Peloquin[10], Steven P. Rowe[6], Tawanda Gumbo[5], Vijay D. Ivaturi[4], Sanjay K. Jain[1,2,3,6*]

[1]Center for Infection and Inflammation Imaging Research, Johns Hopkins University School of Medicine, Baltimore, MD, USA
[2]Center for Tuberculosis Research, Johns Hopkins University School of Medicine, Baltimore, MD, USA
[3]Department of Pediatrics, Johns Hopkins University School of Medicine, Baltimore, MD, USA
[4]Center for Translational Medicine, University of Maryland School of Pharmacy, Baltimore, MD, USA
[5]Center for Infectious Diseases Research and Experimental Therapeutics, Baylor University Medical Center and Texas Tech University Health Sciences Center, Dallas, TX, USA
[6]Russell H. Morgan Department of Radiology and Radiological Sciences, Johns Hopkins University School of Medicine, Baltimore, MD, USA
[7]Department of Anesthesiology and Critical Care Medicine, Johns Hopkins University School of Medicine, Baltimore, MD, USA
[8]Department of Medicine, Johns Hopkins University School of Medicine, Baltimore, MD, USA
[9]Vaccine and Infectious Disease Division, Fred Hutchinson Cancer Research Center, Seattle, WA, USA
[10]Infectious Disease Pharmacokinetics Laboratory, Pharmacotherapy and Translational Research, University of Florida College of Pharmacy, Gainesville, FL, USA

*Corresponding author

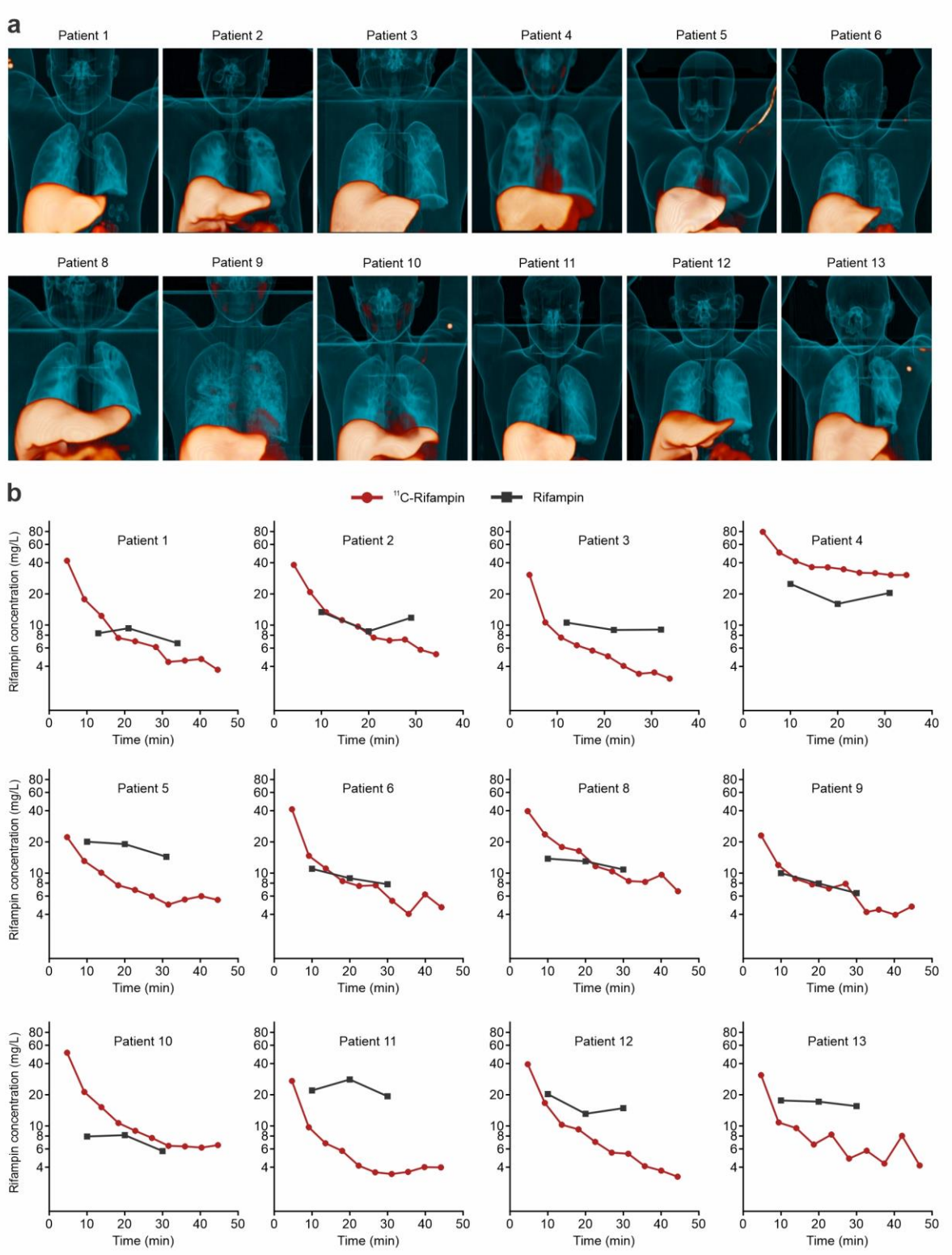

Supplementary Figure 1. ^{11}C-Rifampin PET/CT in TB patients. (a) Three-dimensional maximum intensity projection (MIP) of all participants. The CT is represented in blue while the ^{11}C-rifampin PET signal is represented in orange. (**b**) Excellent matching between dose-normalized plasma ^{11}C-rifampin PET signal and plasma rifampin levels measured using mass spectrometry, obtained on the same day, is shown. The dose normalization of the ^{11}C-rifampin concentrations was made under the assumption of pharmacokinetic linearity across the range of doses from microdose to therapeutic rifampin dosing. Patient 7 was excluded from the study due to significant motion artifact during the ^{11}C-rifampin PET/CT.

Supplementary Table 1. Selection criteria for patient enrollment in the clinical study.

- Greater than or equal to 18 years of age
- Confirmation of *Mycobacterium tuberculosis* by culture or molecular testing (GeneXpert) and susceptible to rifampin
- Imaging evidence demonstrating pulmonary disease and currently being administered a rifampin-based TB drug regimen
- On TB treatment for ≤ 6 weeks by the time of the ^{11}C-rifampin PET/CT. Repeat imaging was also performed in subjects on TB treatment >13 weeks (90 days)
- Not pregnant
- Platelet count > 50,000/mm^3
- Neutrophil count > 1,000/mm^3
- Serum creatinine < 3 times the upper limit of normal
- Total bilirubin < 3 times the upper limit of normal
- Liver transaminases < 5 times the upper limit of normal
- Not treated with an investigational drug, biologic, or therapeutic device within 30 days prior to the ^{11}C-rifampin PET/CT
- Adequate venous access
- Ability to provide written informed consent

Supplementary Table 2. Mass spectrometry results of plasma samples from patients.

Patient ID	Minutes after an IV dose of 600mg of rifampin	Drug concentration (µg/mL)	
		Rifampin	25-Desacetyl Rifampin
1	Pre-dose	Not detected	Not detected
	13	8.32	0.19
	21	9.31	0.35
	34	6.68	0.33
2	Pre-dose	0.02	Not detected
	10	13.37	0.43
	20	8.72	0.30
	29	11.79	0.58
3	Pre-dose	Not detected	Not detected
	12	10.58	0.66
	22	8.97	0.71
	32	9.05	0.78
4	Pre-dose	1.39	0.84
	10	24.98	2.71
	20	16.06	2.18
	31	20.47	3.19
5	Pre-dose	0.12	0.01
	10	20.08	0.93
	20	19.06	1.14
	31	14.36	0.87
6	Pre-dose	0.01	Not detected
	10	10.99	0.31
	20	8.92	0.31
	30	7.79	0.33
8	Pre-dose	Not detected	Not detected
	10	13.78	0.21
	20	13.00	0.22
	30	10.83	0.28
9	Pre-dose	0.04	0.00
	10	9.98	0.31
	20	7.94	0.36
	30	6.42	0.35
10	Pre-dose	0.02	Not detected
	10	7.91	0.31
	20	8.15	0.38
	30	5.73	0.31
11	Pre-dose	Not detected	Not detected
	10	21.98	0.86
	20	28.08	1.32
	30	19.32	1.07
12	Pre-dose	0.04	Not detected
	10	20.29	0.57
	20	13.10	0.46
	30	14.83	0.51
13	Pre-dose	Not detected	Not detected
	10	17.62	0.80
	20	17.15	0.84
	30	15.54	0.86

Supplementary Table 3. Rifampin PK-lung-biodistribution model parameter estimates and 95% confidence interval. n=12 patients**.**

	Unit	Estimate	Between subject variability, BSV (%CV)	95% Confidence interval	
Maximal elimination rate (V_{max})	L/hr/70kg	525 FIX			
Rifampicin concentration at which the elimination is half-maximal (K_m)	mg/L	70 FIX			
Volume of distribution (V_c)	L/70kg	37	40	29	51
Equilibration rate constant between venous and left ventricle compartments ($K_{eq\text{-}lv}$)	/hr	40		38.2	41.8
Partition Coefficient for left ventricle compartment (PC_{LV})		0.38		-1.47	2.23
Equilibration rate constant between venous and lung compartments ($K_{eq\text{-}lung}$)	/hr	42 FIX			
Partition Coefficient for unaffected lung (PC_{UL})		1.2	22	0.88	1.5
Partition Coefficient for pulmonary lesion (PC_{PL})		0.69	23	0.53	0.85
Partition Coefficient for cavity wall (PC_{CW})		0.60	17	0.43	0.77
Clearance for microdose (CL_{mic})	L/hr/70kg	22	21	20.1	23.8
Volume of distribution for microdosing ($V_{c,mic}$)	L/70kg	10	48	8.2	11.8
Maximal increase in the enzyme production rate (S_{max})		1.04 FIX			
Rifampin concentration at which half the S_{max} is reached (SC_{50})	mg/L	0.0705 FIX			
Rate constant for first-order degradation of the enzyme pool (k_{enz})	/hr	0.00369 FIX			
Mean transit time (MTT)	hr	0.713 FIX			

Supplementary Table 4. Simulated rifampin AUC_{0-24} at steady state (ss). Values represent simulation after oral and intravenous (IV) administration of daily doses of rifampin from 10-50 mg/kg in plasma and lung regions based on the PK-lung-biodistribution model. Oral bioavailability was assumed to be 90%. Median, [10^{th}, 90^{th}] percentiles are reported. n=1000 virtual patients generated by Monte Carlo Simulations using the developed lung-biodistribution model.

	Daily dose (mg/kg)	**Plasma $AUC_{24hr,ss}$** (mg·hr/L)	**Unaffected lung $AUC_{24hr,ss}$** (mg·hr/kg)	**Lesion $AUC_{24hr,ss}$** (mg·hr/kg)	**Cavity wall $AUC_{24hr,ss}$** (mg·hr/kg)
Oral	10	50.5 [46.2, 62.8]	16.05 [8.49, 29.9]	8.8 [4.69, 17.32]	7.9 [4.4, 13.41]
	15	77.5 [70.1, 99.4]	23.35 [12.6, 44.41]	13.5 [7.4, 24.83]	12.45 [7.1, 21.62]
	20	104.85 [94.7, 140.06]	33.45 [17.98, 59.61]	18.7 [10.59, 36.81]	16.8 [9.6, 30.3]
	25	134.35 [120.4, 179.83]	41.5 [22.8, 79.62]	23.85 [12.6, 47.51]	21.3 [12, 38.43]
	30	166.65 [147, 235.62]	51.55 [27.8, 95.11]	31.1 [16.6, 58.92]	26.5 [14.9, 49.11]
	35	199.9 [174.59, 276.3]	62.4 [33.27, 117.91]	37.1 [19.1, 70.8]	32.4 [18.2, 56.6]
	40	234.7 [203.19, 337.96]	73.5 [37.1, 152.02]	41.35 [21.3, 85.5]	37.3 [20.59, 69]
	45	268.6 [232.89, 401.98]	87.35 [44.89, 168.76]	49.45 [24.3, 97.52]	42.05 [23.2, 78.91]
	50	306.7 [263.49, 437.42]	99.25 [50.59, 187.13]	55.3 [29.1, 111.77]	48.05 [27.27, 91.4]
IV	10	57 [51.5, 73.5]	17.75 [9.2, 34.14]	10.2 [5.5, 19.1]	9 [5.2, 15.9]
	15	86.9 [78.5, 117.91]	28 [14.89, 52.03]	16.1 [8.1, 29.4]	13.4 [7.8, 24.51]
	20	121 [106.8, 172.81]	38.1 [19.89, 75.94]	21.6 [12.4, 43.36]	18.7 [10.8, 36.63]
	25	156.05 [135.7, 221.22]	49 [26.18, 97.79]	28.2 [15, 56.32]	24.8 [13.8, 43.21]
	30	191.9 [166.28, 275.37]	59.9 [30.95, 119.61]	34.3 [18.3, 69.72]	30.1 [16.79, 54.01]
	35	230.65 [198.79, 346.92]	75.6 [39.16, 145.26]	42.4 [21.6, 91.18]	36.25 [21, 68.5]
	40	273.8 [232, 416.6]	86.2 [45.77, 169.04]	50.05 [24.99, 108.01]	43.65 [24.39, 82.01]
	45	316.95 [268.09, 496.35]	100.9 [53.1, 204.56]	57.65 [29.49, 115.21]	50.35 [28.58, 95.3]
	50	364.2 [302.5, 576.06]	115.3 [59.78, 237.92]	68.4 [33.2, 136.42]	58.65 [32.84, 118.4]

Supplementary Table 5. Injected dose and tissue AUC ratios derived from ^{11}C-rifampin PET. Rifampin area under the concentration-time curves (AUC) were obtained by integrating the area under the dynamic ^{11}C-rifampin PET time-activity curves and the tissue AUC ratio (tissue to plasma) calculated for all patients.

Participant number	Injected mass (ng)	AUC (ng·h/g)				AUC ratio to plasma		
		Plasma	Cavitary wall	Lesions	Unaffected lung	Cavitary wall	Lesions	Unaffected lung
1	1322.10	75.33	-	26.37	54.94	-	0.35	0.73
2	3051.48	138.56	-	68.07	149.66	-	0.49	1.08
3	940.42	27.08	6.64	7.47	25.12	0.25	0.28	0.93
4	749.66	103.84	30.56	30.70	82.84	0.29	0.30	0.80
5	1134.77	51.00	-	-	39.51	-	-	0.77
6	1030.64	56.73	17.50	22.48	40.61	0.31	0.40	0.72
8	537.51	39.75	-	10.52	20.38	-	0.26	0.51
9	608.41	25.61	9.06	16.44	19.90	0.35	0.64	0.78
10	725.35	51.15	-	19.54	46.33	-	0.38	0.91
11	1551.15	54.17	13.26	16.72	25.20	0.24	0.31	0.47
12	2043.49	108.96	49.16	48.08	77.56	0.45	0.44	0.71
13	1335.98	73.17	-	33.68	44.34	-	0.46	0.61

Supplementary Table 6. Digitized data used for external validation. The PK model was externally validated using digitized data from 14 studies with TB patients.

Publication	Year	Population
Loos *et al. Klin Wochenschr*	1985	Adults
Koup *et al. Ther Drug Monit*	1986	Children
Ruslami *et al. Antimicrob Agents Chemother*	2007	Adults
Schaaf *et al. BMC Med*	2009	Children
Thee *et al. Antimicrob Agents Chemother*	2011	Children
Ruslami *et al. Lancet Infect Dis*	2013	Adults
Ramachandran *et al. Int J Tuberc Lung Dis*	2013	Children
Hiruy *et al. J Antimicrob Chemother*	2015	Children
Boeree *et al. Am J Respir Crit Care Med*	2015	Adults
Chigutsa *et al. Antimicrob Agents Chemother*	2015	Adults
Kwara *et al. J Pediatric Infect Dis Soc*	2016	Children
Swaminathan *et al. Clin Infect Dis*	2016	Children
Bekker *et al. Antimicrob Agents Chemother*	2016	Children
Boeree *et al. Lancet Infect Dis*	2017	Adults